JOURNAL OF SOLID STATE CHEMISTRY 98, 404–414 (1992)

Evolution of the Crystal Field Effects in (La,Gd)OBr : Eu^{3+} Series

HANS-JÜRGEN LIMBURG

Leuchtstoffe und Feinchemikalien GmbH, O-6202 Bad Liebenstein, Germany

JORMA HÖLSÄ AND PIERRE PORCHER*

Department of Chemical Engineering, Helsinki University of Technology, SF-02150 Espoo, Finland

AND GERHARD HERZOG, DETLEF STARICK, AND HARM WULFF

Sektion Chemie der Ernst-Moritz-Arndt-Universität Greifswald, O-2200 Greifswald, Germany

Received August 19, 1991; in revised form December 18, 1991

A complete series of gadolinium-substituted lanthanum oxybromides doped with Eu^{3+} ion, $(La_{1-x}Gd_x)OBr:Eu^{3+}$ $(0 \leq x \leq 1)$, were prepared and characterized by X-ray powder diffraction (XRD) and photoluminescence spectroscopy. The XRD analyses revealed the complete solid solubility between La^{3+} and Gd^{3+} host cations. The luminescence spectra of $(La_{1-x}Gd_x)OBr:Eu^{3+}$ powder samples were recorded at 21 K between 475 and 770 nm (13,000 and 21,000 cm^{-1}). The $^5D_{0-1} \rightarrow {}^7F_{0-4}$ transitions were analyzed and the $^7F_{0-4}$ energy level schemes were assigned according to the selection rules between the crystal field (c.f.) sublevels of the $^5D_{0-1}$ and $^7F_{0-4}$ levels for the C_{4v} point symmetry of the RE^{3+} site in the *RE* oxybromides. The spectral analysis confirmed the formation of complete La–Gd solid solutions except for the splitting of a few *E* levels. These splittings were concluded to result from a decrease in the site symmetry from C_{4v} to C_{2v} owing to the ordered substitution of the La^{3+} ions with Gd^{3+}. The c.f. analysis yielded sets of five nonzero B_q^k parameters which reproduced the experimental $^7F_{0-4}$ energy level schemes within rms deviations between 5 and 8 cm^{-1}. The parameters vary smoothly (except the B_0^6 parameter) as a function of the Gd content. The c.f. parameter sets calculated by using the electrostatic point charge model showed no correlation to the phenomenologically determined sets. The electrostatic model must thus be considered inadequate to account for the interactions in *RE* oxybromides. © 1992 Academic Press, Inc.

I. Introduction

The PbFCl-type phosphors, i.e., RE^{3+} activated rare earth oxyhalides (*REOX*) and RE^{2+} activated barium fluoro halides (Ba*FX*), have received considerable industrial attention in the past 10 years. The RE^{3+} and especially the Eu^{3+} and Tb^{3+} activated *REOX* compounds have also provided convenient scientific approach to study the luminescence properties of rare earth ions in solids and the influence of the crystal field. Crystal field (c.f.) analyses have been conducted on *RE*OCl : Eu^{3+}, (*1*) *RE*OBr : Eu^{3+}

* Permanent address: Laboratoire des Elements de Transition dans les Solides, U.P.R. 210, C.N.R.S., 1, Pl. A. Briand, F-92190 Meudon, France.

0022-4596/92 $5.00

(*2*) and *RE*OCl : Tb^{3+} (*3*) (*RE* = Y, La, and Gd), and *RE*OCl : Pr^{3+} (*RE* = La, Y, Gd, and Y) (*4*). Recently the EuOCl system has been studied, too (*5*). Also the *M*FCl : Sm^{2+} (*M* = Sr and Ba) system has been investigated (*6, 7*). The pressure dependence of the c.f. effect on the Eu^{3+} energy level structure in LaOCl has been studied (*8*), too.

Practically in all studies the c.f. effect on the Eu^{3+} ion is investigated by using the ^7F_J basis alone. Only a very few papers dealing with a larger basis set of the $^{2S+1}L_{JM}$ wavefunctions can be found in the literature (*9*). In this study it was shown that the c.f. effect on the ground multiplet, the septet $^7F_{0-6}$, can be carried out in a perfectly adequate manner on this very reduced set. This approximation is justified because of the large gap between the ^7F_J ground multiplet and the rest of the $4f^6$ configuration, primarily the ^5D_J quintet. Furthermore, the c.f. operator mixes only levels of the same spin multiplicity, which leaves only the mixing within the ground septet to be considered.

The previous studies of the *RE* oxyhalide systems displayed considerable variation of the c.f. effect with different host matrix cations and anions. The investigations have, however, dealt only with pure matrix compounds without partial substitution of either the cation of anion sublattice which could enable us to monitor the change in the c.f. strength in a continuous manner. Furthermore, the partial substitution of the cation or anion sublattice may reveal important information about the mutual solid solubility of the trivalent *RE* ions. In this paper we present the results of the c.f. analysis of $(La_{1-x}Gd_x)OBr : Eu^{3+}$ ($0 \leq x_{Gd} \leq 1$) phosphors with partial substitution of the cation host sublattice.

II. Experimental

1. Sample Preparation

The europium-doped $(La_{1-x}Gd_x)OBr$ phosphors used in this investigation were prepared by the reaction of corresponding RE_2O_3 mixtures with NH_4Br at 450°C followed by a $REBr_3$/KBr flux recrystallization process in an inert atmosphere at a temperature between 850 and 1000°C (*10*). The recrystallization temperature was varied in order to obtain similar particle size distribution in all phosphor samples. The nominal Eu^{3+} activator concentration was 2.5 mole%. The details of the preparation procedure have been described elsewhere (*11*). The purity of the products was controlled with X-ray powder diffraction, which showed no presence of other phases. Nevertheless, the rather large width of the X-ray diffraction peaks indicates some disturbance of the lattice structure.

2. Optical Measurements

The luminescence spectra were obtained at 21 K between 13,000 and 21,000 cm^{-1} under UV excitation. The experimental apparatus consisted of an UV excitation source, a liquid hydrogen cryostat with the sample, a Carl–Zeiss–Jena GDM 1000 double monochromator, and a photomultiplier, with appropriate amplification and recording facilities. The spectral resolution achieved with this apparatus was better than 2 cm^{-1}.

The luminescence was excited by a low-pressure mercury discharge lamp emitting mainly the 253.7 nm line. The lines in the visible range were filtered out to a high degree. The remaining weak lines were used for the exact calibration of the wavelength scale used.

III. Results and Discussion

1. Crystal Structure of RE Oxybromides

The whole *RE* oxybromide series crystallizes with the tetragonal PbFCl-type structure with space group $P4/nmm$–D^7_{4h}, (No. 129 in (*12*)) and $Z = 2$ (*13*). The *RE* atoms occupy a single site with C_{4v} point symme-

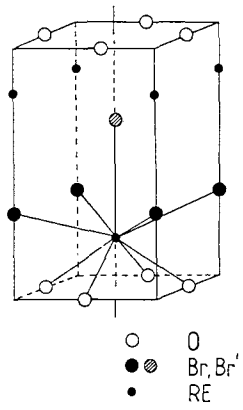

FIG. 1. Crystal structure of *RE*OBr.

try. The *RE* oxybromides have the typical layered *RE* oxysalt structure with distinct covalent $(REO)_n^{n+}$ complex cation and anion layers (*14*, *15*). The coordination polyhedron resulting from a ninefold coordination to four oxygen and five bromine atoms is a regular monocapped tetragonal antiprism (Fig. 1). Because of the structural arrangement of this kind the anisotropy of the lattice is high.

Due to the small differences in the ionic radii between La^{3+} and Gd^{3+} ions the $(La_{1-x}Gd_x)OBr$ series could be expected to form solid solution for any composition. Indeed, the absence of other phases as deduced from the X-ray analyses supports the complete solid solubility over the $(La_{1-x}Gd_x)OBr$ series. Usually when no complete solid solubility exists the lattice parameters show some discontinuity. In the *RE*OBr case the lattice parameters vary smoothly through the whole series as a function of the Gd-content (Fig. 2). The evolution of the *a* and *c*-dimensions are opposite to each other, resulting in an almost constant volume of the unit cell.

The lattice parameters and calculated atomic distances for the $(La_{1-x}Gd_x)OBr$ series are summarized in Table I. The substitution of La by Gd results in a considerable elongation of the unit cell in the direction of the fourfold symmetry axis parallel to the crystallographic *z*-axis. The *RE*–Br′ distance (cf. Fig. 1) increases strongly from 3.480 to 4.206 Å, whereas the other *RE*–Br and *RE*–O distances decrease only by 0.112 and 0.128 Å, respectively, which corresponds well to the difference in the radius between the La^{3+} and Gd^{3+} ions. As far as the immediate coordination sphere of the *RE* atoms is considered this evolution results in the decrease of the coordination number of 9 for the La^{3+} ion to 8 for the Gd^{3+} one. On the other hand, the structural modifications incite also a decrease in the anisotropy of the crystal lattice and thus the polarizability of the RE^{3+} ion should be reduced.

2. *Spectral Analysis*

In the wavelength range studied the emission spectra of the Eu^{3+} ion in $(La_{1-x}Gd_x)OBr$ consist of up to 80 lines (Fig. 3). The lines can be attributed to the transitions between the Stark sublevels of the ^5D_J (J = 0–2) and ^7F_J (J = 0–6) levels. These

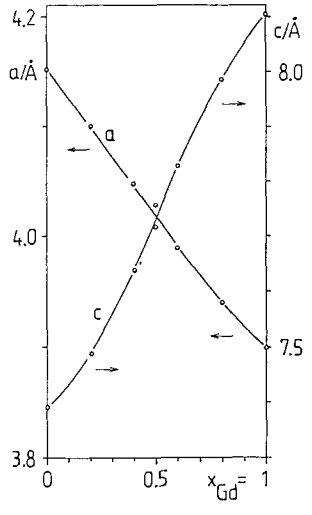

FIG. 2. Evolution of the unit cell dimensions of $(La_{1-x}Gd_x)OBr$.

TABLE I

UNIT CELL DIMENSIONS AND ATOMIC DISTANCES OF THE $(La_{1-x}Gd_x)OBr$ SERIES (IN Å)

	$(La_{1-x}Gd_x)OBr$						
	$x = 0.0$	0.2	0.4	0.5	0.6	0.8	1.0
a	4.1525(1)	4.1005(4)	4.048(1)	4.0290(5)	3.9894(8)	3.9401(8)	3.8993(8)
c	7.3894(7)	7.488(1)	7.639(3)	7.715(2)	7.830(7)	7.987(2)	8.105(2)
RE–O	2.404	2.374	2.350	2.340	2.325	2.301	2.276
RE–Br	3.290	3.263	3.239	3.232	3.217	3.196	3.178
RE–Br′	3.480	3.594	3.732	3.804	3.895	4.043	4.174

transitions are mainly of electric dipole character except for the $^5D_0 \rightarrow {}^7F_1$ magnetic dipole transition. However, other transitions possess significant magnetic dipole contribution, too. The number and symmetry labels of the c.f. levels for each ^7F_J level as well as the selection rules for the electric and magnetic dipole transitions from the ^5D_J levels for the C_{4v} symmetry have been summarized in (*1*).

Transitions from the $^5D_0$ level to the ^7F_J ($J = 0$–4) ones are the most intense ones and in general easy to assign. Accordingly, only these lines were used to construct the ^7F_J energy level scheme. In a few cases (the $^7F_3$ levels) the emission from the $^5D_1$ levels were used. Usually it was not possible to detect any transitions to the *B* sublevels of the $^7F_2$ level. Transitions to the $^7F_5$ sublevels as well as most of the transitions from the $^5D_1$ and $^5D_2$ levels were, especially for the substituted compounds, either very weak or difficult to assign reliably owing to overlap with other lines.

The observed $^5D_0 \rightarrow {}^7F_{0-4}$ and $^5D_1 \rightarrow {}^7F_3$ transitions in the $(La_{1-x}Gd_x)OBr:Eu^{3+}$ emission spectra are summarized in Table II as a function of the Gd content. The ener-

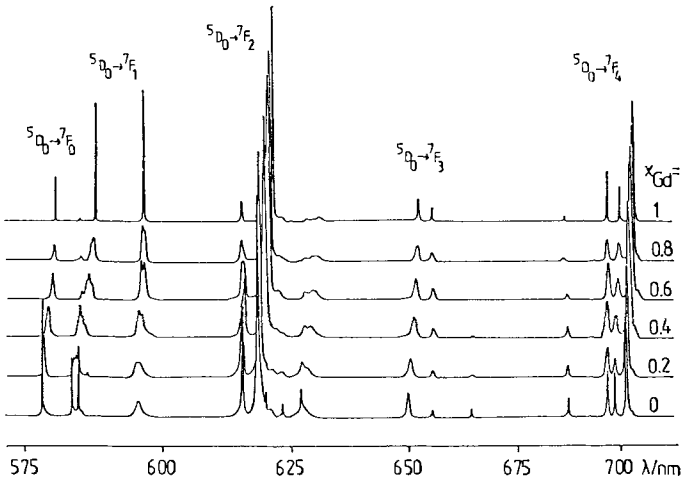

FIG. 3. The emission spectra of $(La_{1-x}Gd_x)OBr:Eu^{3+}$ at 21 K between 575 and 715 nm (14,000 and 17,500 cm^{-1}).

TABLE II

ENERGIES OF SELECTED LINES IN THE EMISSION SPECTRA OF THE $(La_{1-x}Gd_x)OBr:Eu^{3+}$ SERIES AT 21 K (IN cm^{-1})

Transition	$(La_{1-x}Gd_x)OBr$						
	$x = 0.0$	0.2	0.4	0.5	0.6	0.8	1.0
$^5D_0 \rightarrow {}^7F_4\ A_1 \rightarrow B''$							
$A_1 \rightarrow B'$	14226	14216	14203	14199	14191		
$A_1 \rightarrow E$	14253	14248	14239	14235	14231	14219	14216
$A_1 \rightarrow A_1$	14312	14307	14304	14301	14292	14290	14283
$A_1 \rightarrow E$	14347	14348	14349	14348	14350	14350	14348
$A_1 \rightarrow A_2$	14435		14423	14419		14407	
$A_1 \rightarrow A_1$	14550	14551	14552	14553	14559	14568	14571
$^5D_0 \rightarrow {}^7F_3\ A_1 \rightarrow B'$						15163	
$A_1 \rightarrow B''$						15209	
$A_1 \rightarrow E$	15265	15265[i]	15267[m]	15269[i]	15269[i]	15269	15269
$A_1 \rightarrow E$	15392	15384[i]	15370[m]	15365[i]	15356[i]	15345	15337
$A_1 \rightarrow A_2$		15403		15396			
$^5D_0 \rightarrow {}^7F_2\ A_1 \rightarrow B'$							
$A_1 \rightarrow A_1$	16178	16166	16152	16142	16133	16118	16103
$A_1 \rightarrow B''$		16287					
$A_1 \rightarrow E$	16254	16254[i]	16256[m]	16256[m]	16257[m]	16257[i]	16261
$^5D_0 \rightarrow {}^7F_1\ A_1 \rightarrow E$	16795	16796[m]	16790[m]	16783[m]	16777[m]	16771[m]	16767
$A_1 \rightarrow A_2$	17140	17116	17091	17071	17066	17031	17017
$^5D_0 \rightarrow {}^7F_0\ A_1 \rightarrow A_1$	17303	17292	17279	17268	17254	17239	17229
$^5D_1 \rightarrow {}^7F_3\ E \rightarrow B'$	16953	16944					
$A_2 \rightarrow E$	16965	16965				16981	16982
$E \rightarrow E$	17047				17047	17043	
$A_2 \rightarrow E$	17091	17089	17077			17071	
$A_2 \rightarrow A_2$	17105	17104	17104	17102	17100	17099	17096

Note. m = mean value of a split line; i = indication of splitting.

gies of the transitions clearly decrease with increasing Gd content as a result of the nephelauxetic effect in agreement with the size of the host cation. Similar decrease in the c.f. splittings of the ^7F_J levels can be observed, too. With increasing Gd content the lines broaden considerably, attaining the maximum at about $x_{Gd} = 0.5$, while narrowing again beyond this concentration. Since no splitting of the singlet to singlet (especially the extremely sharp $^5D_0 \rightarrow {}^7F_0\ A_1 \rightarrow A_1$) transitions can be observed, the increase in the linewidths can attributed to the increased inhomogeneous broadening due to inevitable distortions in the crystal lattice resulting from the gradual substitution of the La^{3+} host cation with Gd^{3+}.

In addition to the large inhomogeneous broadening of the emission lines, the transitions to the E sublevels of the $^7F_{1,2}$ levels show slight splitting in the Gd concentration range $0.4 \leq x_{Gd} \leq 0.6$ as shown in Fig. 4 for the $^5D_0$–$^7F_2$ transition. The reason for the splittings is evidently a decrease in the RE^{3+} site symmetry from C_{4v} probably to C_{2v} due to the distortions in the host lattice caused by the ordered substitution of the La^{3+} sites by Gd^{3+} ions.

The experimental Stark levels of the ^7F_J ($J = 1$–4) levels (Table III) were obtained from the careful interpretation of the corresponding emission spectra according to the group theoretical selection rules. The levels were labeled with the appropriate irreduc-

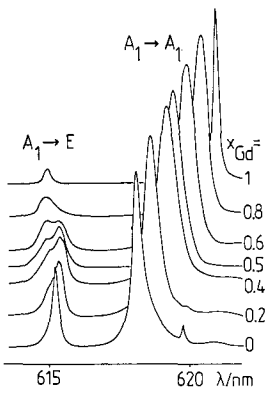

FIG. 4. The $^5D_0 \rightarrow {}^7F_2$ transition of $(La_{1-x}Gd_x)OBr:Eu^{3+}$ at 21 K.

ible representations of the C_{4v} point group. However, the two groups of B levels, B' and B'', may be assigned either to the B_1 or B_2 representation. The Stark-level positions vary smoothly as a function of the Gd content (Fig. 5). In general the c.f. splittings of the $^7F_{0-4}$ levels tend to decrease from the LaOBr to the GdOBr host. Furthermore, the energy level schemes suggest that, for the $^7F_{2,3}$ levels, two Stark levels might cross which, in the case of levels possessing similar symmetry properties, might cause severe repulsion. However, no such effects can be observed in the energy level schemes.

3. Theoretical Considerations

The c.f. effect on the energy level scheme of the RE^{3+} ions is rather small and can usually be considered as a minor perturbation in the free-ion scheme. The most convenient and also most used approach to describe the c.f. effect is the phenomenological one when taken into account the high number of electrons in RE systems. According to this approach the c.f. effect is studied with the aid of the c.f. parameters completely derived from the experimentally

TABLE III

OBSERVED AND CALCULATED ENERGY LEVELS OF THE Eu^{3+} ION IN THE $(La_{1-x}Gd_x)OBr$ SERIES (IN cm^{-1})

	$(La_{1-x}Gd_x)OBr:Eu^{3+}$													
	x = 0.0		0.2		0.4		0.5		0.6		0.8		1.0	
Level	Exp.	Calc.	Exp.	Calc.	Exp.	Calc.	Exp.	Calc.	Exp.	Calc.	Exp.	Calc.	Exp.	Calc.
$^7F_0$ A_1	0	0	0	0	0	0	0	0	0	0	0	0	0	0
$^7F_1$ A_2	163	153	176	168	188	176	197	184	194	186	208	199	212	209
E	508	513	496	500	489	495	485	490	477	481	468	473	462	464
$^7F_2$ B''		1001	1005	1006		1003		1009		993		992		998
E	1049	1045	1038	1037	1023	1018	1013	1008	997	994	982	979	968	965
A_1	1125	1134	1126	1136	1127	1137	1126	1135	1121	1126	1121	1129	1126	1128
B'		1410		1407		1385		1362		1356		1334	1299	1302
$^7F_3$ A_2	1900	1903	1889	1895	1876	1886	1872	1879	1865	1869	1854	1858	1847	1854
E	1911	1914	1908	1912	1909	1913	1903	1910	1898	1901	1894	1857	1892	1897
B''	2021	2023		2020		2031		2036	2024	2026	2030	2033		2041
E	2038	2035	2027	2020	2012	2007	1999	1993	1985	1983	1970	1966	1960	1952
B'	2138	2132		2110	2116	2111	2104	2096	2092	2084	2076	2071		2055
$^7F_4$ A_1	2753	2754	2741	2744	2727	2728	2715	2714	2695	2694	2671	2672	2658	2657
A_2	2868	2871		2882	2856	2867	2849	2856		2850	2832	2838		2828
E	2956	2950	2944	2933	2930	2922	2920	2915	2904	2897	2889	2886	2881	2882
A_1	2991	2993	2985	2992	2975	2972	2967	2967	2957	2958	2949	2950	2946	2948
E	3050	3054	3044	3050	3040	3046	3033	3036	3023	3025	3021	3019	3013	3012
B'	3077	3076	3076	3075	3076	3076	3069	3067	3063	3060	3057	3055	3060	3059
B''		3118		3112	3125	3119		3097		3095	3078	3079		3061
$^5D_0$ A_1	17303		17292		17279		17268		17254		17239		17229	
$^5D_1$ A_2	19005		18998		18982		18979		18965		18953		18943	
E	19091				19067				19032		19016			

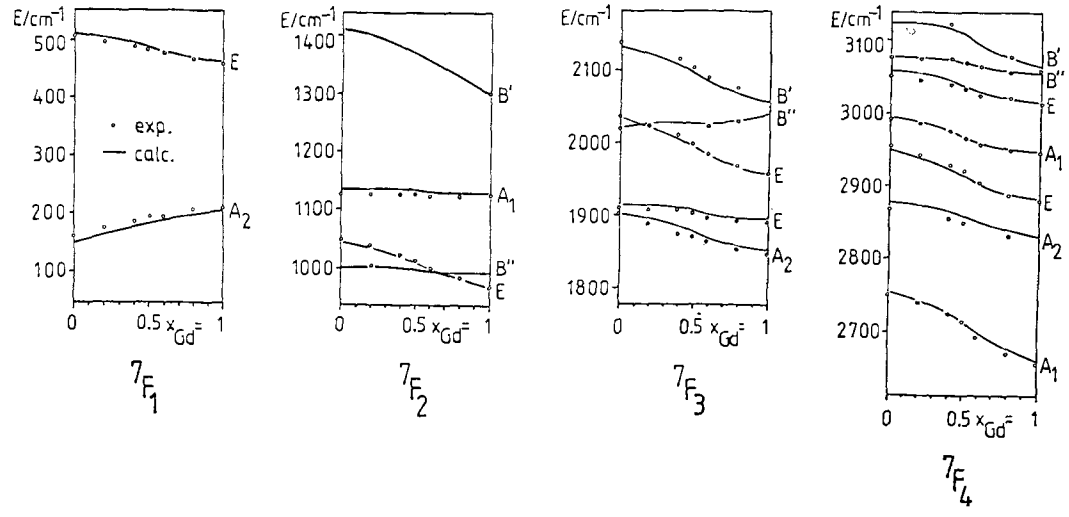

FIG. 5. Crystal field splitting of the $^7F_{1-4}$ levels in $(La_{1-x}Gd_x)OBr:Eu^{3+}$.

known energy level scheme of the RE^{3+} ion. However, there exist other, more theoretical approaches, which due to the heavy electron configuration of these ions, employ more or less severe approximations to describe the c.f. effect. In this work we start with the phenomenological determination of the c.f. B_q^k parameters from the $^7F_{0-4}$ energy level scheme and to compare these values with those obtained by the electrostatic point charge model.

3.1. Phenomenological model. Following Wybourne's formalism (*16*) the c.f. Hamiltonian H_{CF} can be expressed as a sum of products between the real and imaginary c.f. parameters (B_q^k and S_q^k) and tensor operators (C_q^k),

$$H_{CF} = \sum_{kq} [B_q^k(C_q^k + (-1)^q C_{-q}^k) + iS_q^k(C_q^k - (-1)^q C_{-q}^k)], \quad (1)$$

where the tensor operators C_q^k are related to the spherical harmonics Y_q^k by the expression

$$C_q^k = (4\pi/(2k+1))^{1/2} Y_q^k. \quad (2)$$

3.2. Electrostatic point charge model. The ab initio calculations can not be performed on such heavy systems as the *RE* ions and thus some approximations must be applied to simplify the model used. The simplest one is the electrostatic point charge model which accounts only for the Coulombic interactions between the ions thus neglecting completely the "covalent" effects. According to this model the c.f. parameters can be calculated as the product of the lattice sums A_q^k and the radial integrals $\langle r^k \rangle$ as follows:

$$B_q^k = A_q^k \cdot \langle r^k \rangle (1 - \sigma_k)\tau^{-k}. \quad (3)$$

In order to consider the covalency this model can be modified by the application of several factors: the lattice sums can be modified by taking into account the effective charges of the ions in contrast to their traditional constant valency. The doping ion—anion distances can also be modified to account for the modifications in the crystal lattice introduced by the doping. Finally, the radial integrals $\langle r^k \rangle$ for the free ion case can be modified for the screening effect of the $4f$ orbitals in the solid state by other orbitals (factors σ_k) and for the expansion

(factor τ). In our calculations only the latter corrections for the radial integrals were applied. The values for the Hartree–Fock radial integrals were obtained from (*17*); those for the screening factors ($\sigma_2 = 0.686$, $\sigma_4 = 0.139$, and $\sigma_6 = -0.109$) from (*18*) and that for the expansion factor $\tau(= 0.845)$ from (*19*).

4. *Crystal Field Simulation*

For the C_{4v} symmetry the c.f. Hamiltonian H_{CF} comprises five nonzero B_q^k parameters:

$$H_{CF} = B_0^2 C_0^2 + B_0^4 C_0^4 + B_4^4 (C_{-4}^4 + C_4^4) + B_0^6 C_0^6 + B_4^6 (C_{-4}^6 + C_4^6). \quad (4)$$

Optimization of the phenomenological c.f. parameters was carried out by minimizing the r.m.s. deviation σ between the experimental and calculated level energies (Eq. 5) using the matrix diagonalization and least squares refinement program GROMINET:

$$\sigma = [\Sigma(E_{exp} - E_{calc})^2/(N_{lev} - N_{par})]^{1/2}. \quad (5)$$

Because of the limited amount of experimental data for the excited multiplets, no attempt was made to simulate the free ion parameters. The basis set of levels for the c.f. calculations and the optimization of the B_q^k parameters was thus restricted to the 49 $^7F_{JM}$ levels. In order to compensate for neglecting the free ion effects and also to avoid the distorting effect of this omission to the c.f. parameterization, the barycenters of the $^7F_{0-4}$ Stark levels were adjusted to correspond to the experimental values. The J-mixing of the $^7F_{JM}$ wavefunctions always included in the calculations rendered the crystal quantum number μ as the only "good" one. For the initial least square refinement with $x_{Gd} = 0$ the B_q^k parameter set obtained in (*2*) were used as a starting set. For cases with $x_{Gd} > 0$, the initial B_q^k parameter set used was obtained from the results of the immediately preceding refinement of the energy level scheme of the sample with lower x_{Gd} value.

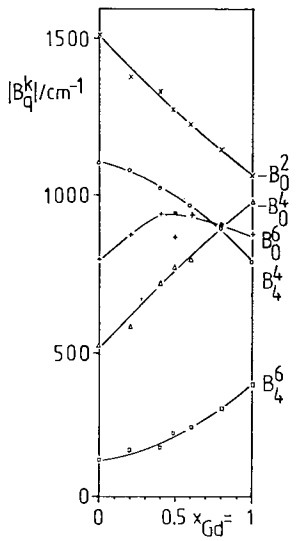

FIG. 6. Evolution of the B_q^k crystal field parameters in the $(La_{1-x}Gd_x)OBr:Eu^{3+}$ series.

For all Gd concentrations the sets of the B_q^k parameters reproduce the experimental $^7F_{0-4}$ energy level schemes in a completely satisfactory manner with the rms deviations between 5 and 8 cm^{-1} (Table III and Fig. 5). The rms deviations tend to be the lowest at the end and the beginning of the series, i.e., for the pure compounds, and attain the maximum in the middle of the series. This might be connected to the increased distortions at the range $x_{Gd} = 0.5$. The estimated standard deviations of the B_q^k values behave in a similar way.

The B_q^k parameters vary quite smoothly—even linearly—as a function of the Gd-content (Table IV and Fig. 6). The only exception is the B_0^6 parameter showing irregular behavior. This parameter is also the least well defined with the largest standard deviation due to the lack of observation of certain c.f. levels of the $^7F_3$ level. The variation of the c.f. parameters is in most cases surprisingly strong, taking into ac-

TABLE IV

CRYSTAL FIELD PARAMETERS OF THE $(La_{1-x}Gd_x)OBr:Eu^{3+}$ SERIES (IN cm^{-1})

Crystal field parameters	$(La_{1-x}Gd_x)OBr:Eu^{3+}$						
	$x = 0.0$	0.2	0.4	0.5	0.6	0.8	1.0
B_0^2 Lattice sum	−1135	−1195	−1156	−1154	−1059	−1009	−1026
Calc.	−458	−482	−466	−466	−427	−407	−414
Exp.	−1515	−1374	−1335	−1271	−1231	−1148	−1064
B_0^4 Lattice sum	−201	−219	−241	−249	−269	−292	−309
Calc.	−685	−746	−823	−851	−917	−995	−1053
Exp.	−524	−582	−721	−779	−794	−908	−981
B_4^4 Lattice sum	185	198	205	209	212	221	235
Calc.	631	675	699	714	722	753	802
Exp.	±1105	±1082	±1024	±938	±969	±902	±791
B_0^6 Lattice sum	13.6	14.8	15.6	16.0	16.6	17.6	19.0
Calc.	376	406	431	442	457	485	523
Exp.	794	871	939	868	937	908	875
B_4^6 Lattice sum	14.1	15.4	16.7	17.3	18.3	19.8	21.4
Calc.	388	424	461	475	504	545	587
Exp.	±160	±192	±197	±255	±264	±325	±403
S	521	496	490	467	469	453	431
σ	6	7	8	8	5	5	5

count the same crystal structure of all RE oxybromides. As discussed in Section III.1, the polarizability of the RE^{3+} ion is, however, considerably modified by the change in the coordination of the RE^{3+} cation to the fifth bromine from LaOBr to GdOBr. Accordingly, though the $(REO)_n^{n+}$ complex cation still determines the general appearance of the c.f. effect (*20–23*), the strength of the effect seems to depend on the anion configuration. In line with this conclusion the c.f. strength parameter S (*24*) decreases strongly with increasing Gd-content (Fig. 7). The c.f. strength parameter S enables the comparison of the c.f. effect between different compounds irrespective of the site symmetry of the RE^{3+} ion (and thus the number of B_q^k parameters).

Experimentally it was found that the E and B'' levels of the $^7F_2$ and $^7F_3$ levels change positions from $LaOBr:Eu^{3+}$ to $GdOBr:Eu^{3+}$. In both cases the c.f. simulation confirms the crossover. Since these levels have different symmetry properties no repulsion could be observed.

Due to the splitting of the E sublevels of the $^7F_{1,2}$ levels in the Gd concentration range $0.4 \leq x_{Gd} \leq 0.6$, the c.f. calculations were carried out on the basis of C_{2v} symmetry. Since the actual splitting of the E levels was

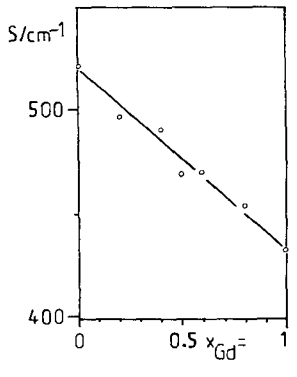

FIG. 7. Evolution of the crystal field strength parameter S in the $(La_{1-x}Gd_x)OBr:Eu^{3+}$ series.

of the order of 15 cm^{-1}, the actual B_2^2 and B_2^4 parameter values assumed also very low values, 19 and -49 cm^{-1}, respectively, while the other parameter values remained constant. The distortions from the C_{4v} symmetry were thus considered insignificant.

5. Comparison between Phenomenological and Point Charge Models

The B_q^k parameter values calculated with the electrostatic point charge model for the $(La_{1-x}Gd_x)OBr:Eu^{3+}$ series are represented in Table IV. The corrected theoretical values for the pure GdOBr host are rather close to those obtained from the phenomenological approach with the exception of the B_0^2 parameter. This is obvious since this parameter is supposed to absorb the bulk of the "covalent" contributions as discussed earlier (*1, 2*). The success of the simple point charge model for the GdOBr matrix is surprisingly good despite the omission of the higher order electrostatic and "covalent" effects.

The theoretical B_q^k values vary quite smoothly along the (La, Gd)OBr series and for the sixth order parameters (and B_4^4) also the direction of the variation corresponds to the experimental trend. In most cases the magnitude of the change in the theoretical parameter values is, however, considerably lower than in the experimental values. Especially the magnitude and the variation of the large B_0^2 parameter is not reflected by the calculated B_0^2 values. All these discrepancies might be connected—at least in part—to the change in the polarizability of the RE^{3+} ion, which is the highest for the LaOBr host then decreasing toward GdOBr.

As to the individual contributions to the electrostatic B_q^k values from the oxygen, *RE*, and bromine atoms some interesting results were obtained. The most important parameter B_0^2 is mainly determined by the oxygen and *RE* atoms with opposite contributions, however. The B_0^4 and B_4^4 values are determined mainly by the contributions from the oxygens, while the B_0^6 and B_4^6 values are determined completely by the oxygens. According to the electrostatic model not only the absolute values of the B_q^k parameters but also their variation depend on the large differences in the *RE*–Br distance but also on the rather small variations of the *RE*–O distance. Since this theoretical model cannot account for the change in polarizability of the RE^{3+} ion this conclusion should be treated with care.

It must be concluded that the Eu^{3+} energy level scheme cannot be described only by purely electrostatic point charge effects alone. The disagreement between the theoretical B_q^k sets and the experimental ones is probably due to the neglect of the electrostatic contributions of higher order as well as of other than electrostatic effects. Furthermore, the correction factors (σ_k and τ) for the radial integrals are only approximate for the *RE*OBr : Eu^{3+} system.

References

1. J. Hölsä and P. Porcher, *J. Chem. Phys.* **75,** 2108 (1981).
2. J. Hölsä and P. Porcher, *J. Chem. Phys.* **76,** 2790 (1982).
3. J. Hölsä and P. Porcher, *J. Chem. Phys.* **76,** 2798 (1982).
4. E. Antic-Fidancev, J. Hölsä, M. Lemaitre-Blaise, and P. Porcher, *J. Chem. Soc. Faraday Trans.* **87,** 3625 (1991).
5. G. D. Del Cul, G. M. Murray, S. E. Nave, C-T. P. Chang, G. M. Begun, and J. R. Peterson, *Eur. J. Solid State Inorg. Chem.* **28,** 155 (1991).
6. G. Grenet, M. Kibler, A. Gros, J. C. Souillat, and J.-C. Gacon, *Phys. Rev. B* **22,** 5052 (1980).
7. J.-C. Gacon, G. Grenet, J. C. Souillat, and M. Kibler, *J. Chem. Phys.* **69,** 868 (1978).
8. Gin Yuanbin, Liu Shensin, Shen Wufu, Wang Lizhong, and Zon Guangtian, *Physica B* **139 & 140,** 555 (1986).
9. O.-K. Moune-Minn, P. Caro, D. Garcia, and M. Faucher, *J. Less-Common Met.* **163,** 287 (1990) (and references cited therein).
10. D. Starick, L. Schwarz, H. Krah, and G. Herzog, DD 226 900 (1–8–1984).

11. D. STARICK AND G. HERZOG, *Thermochim. Acta* **92,** 473 (1985).
12. D. BROWN, "Halides of Lanthanides and Actinides," Wiley, New York (1968).
13. N. F. M. HENRY AND K. LONSDALE, Eds., "International Tables of X-ray Crystallography," Vol. 1, Kynoch Press, Birmingham (1969).
14. P. CARO, *C.R. Acad. Sci. (Paris) Ser. C* **262,** 992 (1966).
15. P. CARO, *J. Less-Common Met.* **16,** 367 (1968).
16. B. G. WYBOURNE, "Spectroscopic Properties of Rare Earths," Interscience, New York (1965).
17. A. J. FREEMAN AND J. P. DESCLAUX, *J. Magn. Magn. Mater.* **12,** 11 (1979).
18. R. P. GUPTA AND S. K. SEN, *Phys. Rev. A* **7,** 850 (1973).
19. J. DEXPERT-GHYS, M. FAUCHER, AND P. CARO, *Phys. Rev. B* **23,** 607 (1981).
20. P. PORCHER, D. R. SVORONOS, M. LESKELÄ, AND J. HÖLSÄ, *J. Solid State Chem.* **46,** 101 (1983).
21. J. HUANG, J. LORIERS, AND P. PORCHER, *J. Solid State Chem.* **43,** 87 (1982).
22. J. HÖLSÄ AND M. KARPPINEN, *Eur. J. Solid State Inorg. Chem.* **28,** 135 (1991).
23. O.-K. MOUNE-MINN, AND P. CARO, *J. Crystallogr. Spectrosc. Res.* **12,** 157 (1982).
24. N. C. CHANG, J. B. GRUBER, R. P. LEAVITT, AND C. A. MORRISON, *J. Chem. Phys.* **76,** 3877 (1982).